Insights into substrate specificity of archaeal Entner-Doudoroff aldolases: the structures of *Picrophilus torridus* 2-keto-3-deoxygluconate aldolase, and *Sulfolobus solfataricus* 2-keto-3-deoxy(6-phospho)-gluconate aldolase in complex with 2-keto-3-deoxy-6-phosphogluconate.

Journal:	*Biochemistry*
Manuscript ID	bi-2018-00535u.R1
Manuscript Type:	Article
Date Submitted by the Author:	n/a
Complete List of Authors:	Zaitsev, Viatcheslav; University of St Andrews, Biomolecular Sciences Johnsen, Ulrike; Christian-Albrechts Universität Kiel, Reher, Matthias; Christian-Albrechts Universität Kiel Ortjohann, Marius; Christian-Albrechts Universität Kiel Taylor, Garry; University of St Andrews, Danson, Michael; University of Bath, Biology & Biochemistry Schönheit, Peter; Christian-Albrechts Universität Kiel, Institut für Allgemeine Mikrobiologie Crennell, Susan; University of Bath, Biology & Biochemistry

Insights into substrate specificity of archaeal Entner-Doudoroff aldolases: the structures of *Picrophilus torridus* 2-keto-3-deoxygluconate aldolase, and *Sulfolobus solfataricus* 2-keto-3-deoxy(6-phospho)-gluconate aldolase in complex with 2-keto-3-deoxy-6-phosphogluconate.

Viatcheslav Zaitsev[a], Ulrike Johnsen[b], Matthias Reher[b], Marius Ortjohann[b], Garry L.Taylor[a], Michael J. Danson[c], Peter Schönheit[b] and Susan J. Crennell[c]#

Biomolecular Sciences, University of St Andrews, St Andrews, Fife, UK[a]; Institut für Allgemeine Mikrobiologie, Christian-Albrechts-Universität, Kiel, Germany[b]; Department of Biology & Biochemistry, University of Bath, Bath, UK[c].

V.Z. and U.J. contributed equally to this work

Corresponding author: Susan Crennell, S.J.Crennell@bath.ac.uk

Second contributing author: Peter Schönheit peter.schoenheit@ifam.uni-kiel.de

Running title: *Picrophilus* and *Sulfolobus* KDG-Aldolase specificity

Abbreviations.

KDG:	2-keto-3-deoxygluconate
KDPG:	2-keto-3-deoxy-6-phosphogluconate
KDG-aldolase:	2-keto-3-deoxygluconate aldolase
KDGK:	KDG kinase
KD(P)G-aldolase:	2-keto-3-deoxygluconate/2-keto-3-deoxy-6-phosphogluconate aldolase
Pt-KDG-aldolase:	*Picrophilus torridus* KDG-aldolase
RMSD:	Root Mean Square Deviation

Ss-KD(P)G-aldolase: *Sulfolobus solfataricus* KD(P)G-aldolase

Table of Contents graphic (Figure7)

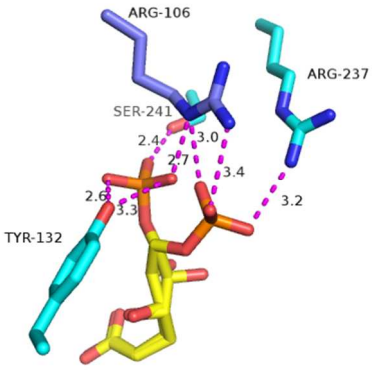

EC number: 4.1.2.51

Keywords: *Picrophilus torridus*, 2-keto-3-deoxygluconate aldolase, crystal structure, enzyme specificity, *Sulfolobus solfataricus*, 2-keto-3-deoxy-phospho-gluconate aldolase, archaeal Entner-Doudoroff pathways

Abstract

The thermoacidophilic archaea *Picrophilus torridus* and *Sulfolobus solfataricus* catabolise glucose via a non-phosphorylative Entner-Doudoroff pathway and a branched Entner-Doudoroff pathway, respectively. Key enzymes for these Entner-Doudoroff pathways are the aldolases, 2-keto-3-deoxygluconate aldolase (KDG-aldolase) and 2-keto-3-deoxy-6-phosphogluconate aldolase (KD(P)G-aldolase). KDG-aldolase from *P. torridus* (Pt-KDG-aldolase) is highly specific for the non-phosphorylated substrate, 2-keto-3-deoxygluconate (KDG), whereas KD(P)G-aldolase from *S. solfataricus* (Ss-KD(P)G-aldolase) is an enzyme catalyzing the cleavage of both KDG and 2-keto-3-deoxy-6-phosphogluconate (KDPG), with a preference for KDPG. The structural basis for the high specificity of Pt-KDG-aldolase for KDG as compared to the more promiscuous Ss-KD(P)G-aldolase has not been analysed before. In the current paper we report the elucidation of the structure of Ss-KD(P)G-aldolase in complex with KDPG at 2.35Å and that of KDG-aldolase from *P. torridus* at 2.50 Å resolution. By superimposition of the active sites of the two enzymes, and subsequent site-directed mutagenesis studies, a network of four amino acids, namely Arg106, Tyr132, Arg237 and Ser241, was identified in Ss-KD(P)G-aldolase that interact with the negatively-charged phosphate group of KDPG, thereby raising the affinity of the enzyme for KDPG. This KDPG-binding network is absent in Pt-KDG-aldolase, which explains the low catalytic efficiency of KDPG cleavage.

Introduction

The discovery of thermophilic micro-organisms has stimulated a wealth of fundamental and applied research into their enzymes, both for the light they may shed on the molecular basis of protein stability and for the potential applications of enzymes with high thermal stability. Most extreme thermophiles are members of the Archaea, the third domain of life, and studies on their metabolic pathways have revealed enzymes with unusual catalytic activities and specificities.

The Archaea degrade glucose and glucose polymers to pyruvate, not via the classical Embden-Meyerhof pathway nor the Entner-Doudoroff pathway reported for Bacteria and Eukarya, but via modifications of these pathways, thereby implicating novel enzymes and enzyme families with unusual catalytic and regulatory features.[1,2,3] Modified Embden-Meyerhof pathways have been described mainly in anaerobic hyperthermophilic archaea whereas aerobic archaea, including the thermoacidophiles *Picrophilus torridus* and *Sulfolobus solfataricus*, degrade glucose via modified versions of the Entner-Doudoroff pathway. For *P. torridus,* growing optimally at 60°C and pH 0.9, a non-phosphorylative Entner-Doudoroff pathway was reported.[4,5] Accordingly, glucose is converted to 2-keto-3-deoxygluconate (KDG) via glucose dehydrogenase and gluconate dehydratase. KDG is then cleaved by a KDG-aldolase to pyruvate and glyceraldehyde, of which the latter is converted to a second molecule of pyruvate via glyceraldehyde dehydrogenase, 2-phosphoglycerate-forming glycerate kinase, enolase and pyruvate kinase (Fig. 1).

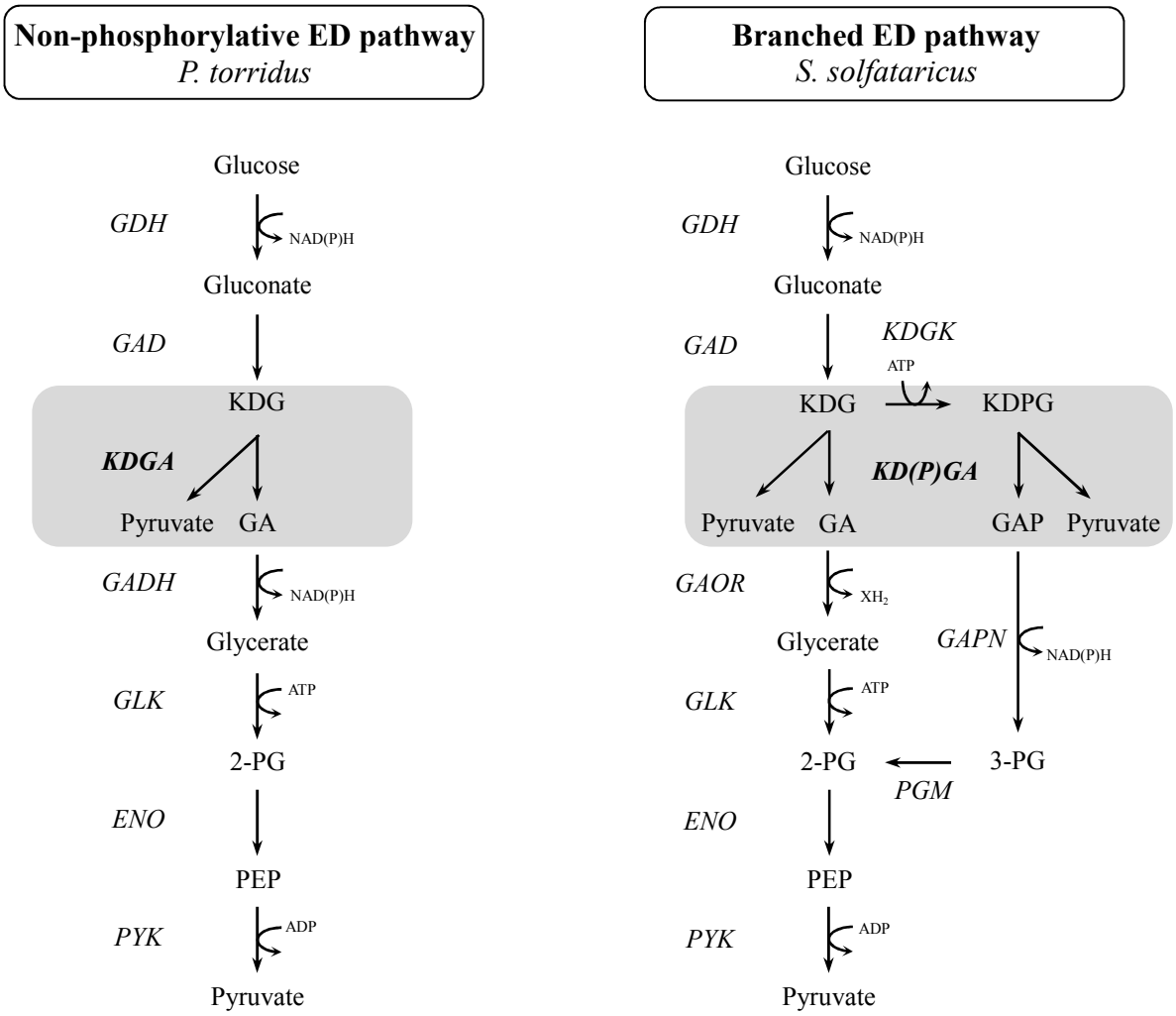

Fig 1 Modified Entner-Doudoroff (ED) pathways in *P. torridus* and *S. solfataricus*. KDG, 2-keto-3-deoxygluconate; GA, glyceraldehyde; 2-PG, 2-phosphoglycerate; PEP, phosphoenolpyruvate; KDPG, 2-keto-3-deoxy-6-phosphogluconate; GAP, glyceraldehyde-3-phosphate; 3-PG, 3-phosphoglycerate; GDH, glucose dehydrogenase; GAD, gluconate dehydratase; KDGA, KDG aldolase; GADH, glyceraldehyde dehydrogenase; GLK, glycerate kinase (2-PG forming); ENO, enolase; PYK, pyruvate kinase; KD(P)GA, KDG/KDPG aldolase; KDGK, KDG kinase; GAOR, glyceraldehyde oxidoreductase; GAPN, non-phosphorylative GAP dehydrogenase; PGM, phosphoglycerate mutase. The C4 epimeric substrate galactose and its respective derivatives of GDH, GAD, KDGK, KDGA and KD(P)GA are not shown.

On the other hand, *S. solfataricus,* growing at 80°C and pH 3.5, possesses a branched Entner-Doudoroff pathway.[6,7] In this pathway, glucose is converted to KDG via glucose dehydrogenase and gluconate dehydratase as in *P. torridus*. Further catabolism of KDG involves two branches; in the first, KDG is cleaved to pyruvate and glyceraldehyde, which is further converted to pyruvate via glyceraldehyde oxidoreductase, glycerate kinase, enolase and pyruvate kinase. In the second branch, KDG is phosphorylated by KDG kinase to generate 2-keto-3-deoxy-6-phosphogluconate (KDPG), which is cleaved to pyruvate and glyceraldehyde-3-phosphate by a KD(P)G-aldolase that catalyzes the cleavage of both KDG and KDPG. Further conversion of glyceraldehyde-3-phosphate to pyruvate involves a non-phosphorylative glyceraldehyde-3-phosphate dehydrogenase, phosphoglycerate mutase, enolase, and pyruvate kinase (Fig. 1).

Both the non-phosphorylative Entner-Doudoroff pathway of *P. torridus* and the branched Entner-Doudoroff pathway of *S. solfataricus* have been described to be promiscuous for the catabolism of both D-glucose and D-galactose .[4,5,7,8]

The substrate specificities of the *Picrophilus* and *Sulfolobus* aldolases are key determinants of their respective metabolic pathways. KDG-aldolase (E.C. 4.1.2.51) from *P. torridus* is highly specific for the substrate KDG, showing up to 2000-fold higher catalytic efficiency compared to KDPG.[4] In contrast, KD(P)G-aldolases are enzymes catalyzing the cleavage of both KDG and KDPG, with a preference for KDPG. KD(P)G-aldolases have been characterized from the *Sulfolobus* species*, S. solfataricus*, *S. acidocaldarius* and *S. tokodaii*, and from *Thermoproteus tenax* .[6,7,9] Both types of aldolases, KDG-aldolase and KD(P)G-aldolase, are Schiff-base-forming class I aldolases that belong to the dihydrodipicolinate synthase-like family of the class I aldolase superfamily, where they form distinct clusters in accordance with their different substrate specificities .[4] It should be noted that the archaeal KDG-aldolase and KD(P)G-aldolase differ from the KDPG aldolases of the classical Entner-Doudoroff pathway of bacteria and of the semi-phosphorylative Entner-Doudoroff pathway of the haloarchaeon *Haloferax volcanii*,[10] which belong to the bacterial type class I KDPG aldolases/4-

hydroxy-2-oxoglutarate aldolase family .[11]

While the differences in substrate specificities of KDG-aldolase and KD(P)G-aldolase are in accordance with their *in vivo* operation in the non-phosphorylative and branched Entner-Doudoroff pathways, respectively, the structural basis for the high specificity of Pt-KDG-aldolase for KDG as compared to the more promiscuous KD(P)G-aldolase from *Sulfolobus* has not been analysed so far. However, the structures of KD(P)G-aldolases from *S. solfataricus* (Ss-KD(P)G-aldolase), *S. acidocaldarius* and *T. tenax* have been determined. KDPG was modelled into the active site of the *S. acidocaldarius* KD(P)G-aldolase [9] and of *T. tenax* KD(P)G-aldolase,[12] and from these structural models two arginines and one tyrosine have been proposed to contact the phosphate group of KDPG.

To analyse the different substrate specificities of the aldolases further, a direct structural comparison of the KDG-aldolase with KD(P)G-aldolase is necessary. Therefore, in the current paper, we report the elucidation of the structure of KDG-aldolase from *P. torridus,* specific for the non-phosphorylated substrate KDG, and also the structure of the KD(P)G-aldolase from *S. solfataricus* in complex with KDPG. By subsequent superimposition of the active sites of the two enzymes, we identify amino acids that contact the phosphate group of KDPG in Ss-KD(P)G-aldolase and the corresponding residues in Pt-KDG-aldolase. Subsequent predictions of the structural basis of the respective substrate specificities are then tested by site-directed mutagenesis.

Materials and Methods

Site-directed mutagenesis

Variants of KDG aldolase from *P. torridus* (Pt-KDG-aldolase) and of KD(P)G aldolase from *S. solfataricus* (Ss-KD(P)G-aldolase) were generated using the QuikChange Lightning Site-directed Mutagenesis Kit (Agilent Technologies, Waldbronn, Germany) or the Q5 Site-directed Mutagenesis Kit (New England Biolabs, Frankfurt, Germany), according to the manufacturers' instructions. The plasmids pET3a-SSO_3197 [8] and pET19b-Pto1279a [4] were used as templates.

Expression and purification of enzymes

Pt-KDG-aldolase and Ss-KD(P)G-aldolase, and their respective variants, were expressed in *E. coli* (DE3) Rosetta pLysS cells grown at 37°C for 4 h in Lysogeny Broth (LB) medium. Expressions were induced by the addition of isopropyl β-D-1-thiogalactopyranoside. Recombinant Pt-KDG-aldolase and variants of the enzyme were purified by heat treatment at 55°C for 30 min, followed by affinity chromatography on Ni-NTA Agarose according to Reher et al. (2010). Eluted KDG-aldolase was then applied to a Superdex 200 HiLoad 16/60 column (GE Healthcare, Freiburg, Germany) that was equilibrated with 50 mM Tris-HCl, pH 7.4, containing 150 mM NaCl. Protein was eluted with an isocratic flow. At this stage, Pt-KDG-aldolase and variants were essentially pure as judged by sodium dodecylsulphate-polyacrylamide gel electrophoresis (SDS-PAGE).

Cell pellets of recombinant Ss-KD(P)G-aldolase and site-directed variants were suspended in 50 mM Tris-HCl, pH 8.6, and passed three times through a French press cell; cell extracts were generated by centrifugation at 39,000 g. Purification was performed by heat treatment at 75°C for 30 min followed by centrifugation at 39,000 g. The resulting supernatant was applied to a Q Sepharose HP HiLoad 16/10 column (GE Healthcare) that was equilibrated in 50 mM Tris-HCl, pH 8.6. The protein was eluted with an increasing gradient from 0 to 2 M NaCl. Fractions containing highest KD(P)G-aldolase activity were applied to a Superdex 200 HiLoad 16/60 column. Elution of protein was performed in 50 mM Tris-HCl, pH 7.4, containing 150 mM NaCl. After this procedure, the protein was

essentially pure as judged by SDS-PAGE.

Determination of enzyme activity

Aldol-cleavage activities of Pt-KDG-aldolase and Ss-KD(P)G-aldolase were measured by following the production of pyruvate from KDG or KDPG. Assays were carried out at 60°C in 50 mM sodium phosphate buffer, pH 6.2, containing 0.3 mM NADH, 3 U lactate dehydrogenase, and KDPG (Sigma-Aldrich, Schnelldorf, Germany; product 79156) or KDG (Sigma-Aldrich, product 12271); the reduction of pyruvate to lactate by NADH, catalysed by lactate dehydrogenase, was monitored spectrophotometrically at 340nm.[4]

Crystallisation, X-ray data collection, processing and model refinement

The genes encoding Pt-KDG-aldolase and Ss-KD(P)G-aldolase were cloned and expressed, and the recombinant enzymes purified and characterised, as described above. For crystallization, Pt-KDG-aldolase was concentrated to 4.2 mg/ml and, following the identification of initial crystallisation conditions (Crystal Screen Cryo HT, Hampton Research), optimal crystals were obtained by the hanging-drop, vapour-diffusion method, using drops of protein and well solution (0.085 M sodium HEPES buffer pH 7.5, 8.5% (v/v) 2-propanol, 17% (w/v) PEG 4000, 15% (v/v) anhydrous glycerol) in equal ratio. Ss-KD(P)G-aldolase, concentrated to 6mg/ml, was also crystallised by the hanging-drop, vapour-diffusion method using drops containing 1.5 μl of protein mixed with 1.5 μl of well solution (0.1M sodium HEPES buffer pH 6.0, 8% (v/v) 2-propanol, 11% (w/v) PEG4000)[13]. The Ss-KD(P)G-aldolase crystals were soaked in well solution containing 15mM KDPG (Sigma) and 20% v/v glycerol (as cryoprotectant) for 5 min, followed by flash-cooling in liquid nitrogen.

X-ray data were collected from Pt-KDG-aldolase crystals at 100K using a Rigaku MicroMax - 007 HF with Saturn 944+ CCD detector. Diffraction spots were visible to at least 2.4Å; however, during data processing the resolution was truncated to 2.5Å to optimise data completeness. X-ray data were processed and scaled using HKL-2000.[14] The molecular replacement pipeline BALBES[15] was used to

find initial phases using the structure of *Bacillus anthracis* 4-hydroxy-tetrahydrodipicolinate synthase DapA-2 (1XKY,[16] with which Pt-KDG-aldolase shares 32% identity) as the search model. Iterative cycles of model building in Coot[17] and refinement in Phenix [18] were required to build a final model.

X-ray data were collected from the SsKD(P)G-aldolase complex crystals at 100K on the I04 beamline at the Diamond Light source, using a Dectris Pilatus 6M-F detector. 720° of data were collected using radiation of wavelength 0.9795Å and processed using DIALS,[19] then scaled using AIMLESS,[20] truncated to 2.35Å to achieve completeness, with high CC(1/2) and sufficient signal (mean I/σ(I)). BALBES[15] was again used to solve the structure, using the unliganded Ss-KD(P)G-aldolase structure (1W37) as the starting model, and cycles of rebuilding in Coot and refinement in Phenix. The KDPG ligand structure was built and the Schiff base conformation and CIF file produced using JLigand.[21]

Except where indicated, PyMOL[22] was used to produce the figures in this paper.

Size-exclusion chromatography

For determination of the native relative molecular masses (M_r) of Pt-KDG-aldolase, Ss-KD(P)G-aldolase and their respective variants, a Superdex 200 HiLoad 16/60 column was calibrated with high-molecular-weight (HMW) and low-molecular-weight (LMW) kits (GE Healthcare, Germany) as specified by the manufacturer. The subunit M_r values were calculated from the protein sequences and were seen to be consistent with estimates from Coomassie-stained SDS-PAGE.

Accession number: The Pt-KDG-aldolase structure has been deposited in the PDB and given the accession number 4UXD, DOI: 10.2210/pdb4uxd/pdb. The Ss-KD(P)G-aldolase structure in complex with KDPG has been given the accession number 6G3Z.

Results and Discussion

Overall Pt-KDG-aldolase structure:

The structure of Pt-KDG-aldolase has been determined to 2.5 Å, deposited in the PDB and given the code 4UXD. Data processing and structure refinement data are given in Table 1. The asymmetric unit contains one Pt-KDG-aldolase tetramer, 19 glycerol (cryoprotectant) molecules, three molecules of propan-2-ol, five of ethane-1,2-diol, two PEG derivatives (PEG, PGE), and 340 water molecules. The structure is of high quality, with a good Molprobity score (1.90, 97th percentile), although 6 residues were classified as Ramachandran plot outliers, these being residue 105 in chains A, C and D, residue 77 in chains A and C, and residue 207 in chain C. All these residues are marginal outliers, not seen in all chains; however, the most consistent outlier is Tyr105 and its unusual conformation can be seen to be caused by its position on the dimer interface, projecting into a pocket in the other monomer (Fig. 2).

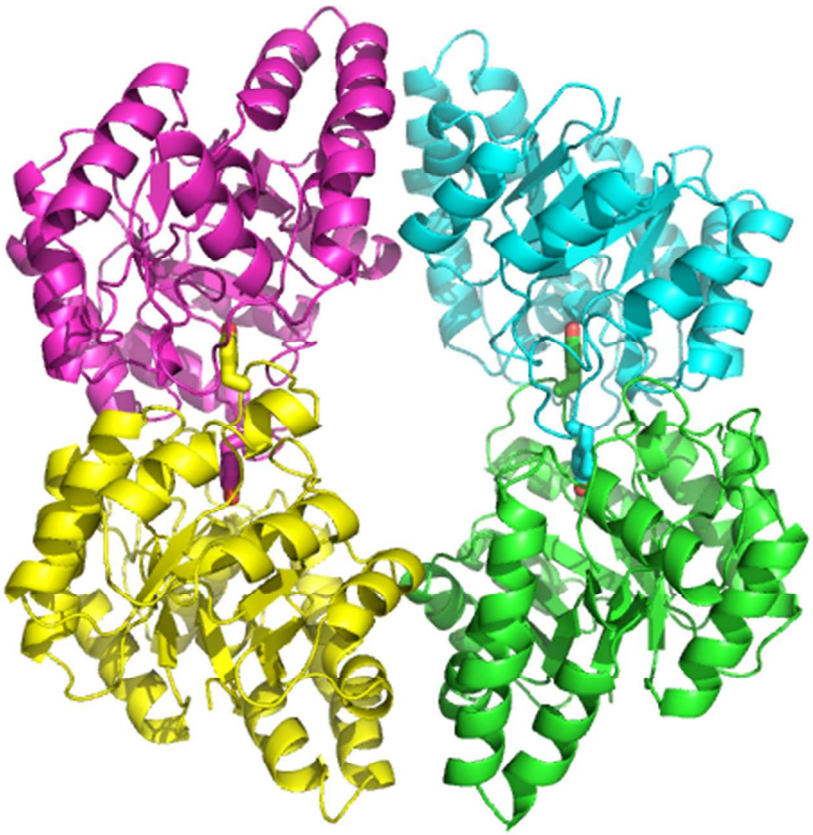

Fig 2: The structure of Pt-KDG-aldolase in cartoon representation, with each monomer in a different colour. The Ramachandran-outliers Tyr 105 are shown in stick form, and can be seen to protrude into a neighbouring molecule as part of the larger dimer interface, the perpendicular tetramer interface being less extensive.

Table 1: Data processing and model refinement statistics. Numbers in parentheses refer to the highest resolution shell in each data set (2.54-2.50Å for Pt-KDG-aldolase, 2.43-2.35Å for Ss-KD(P)G-aldolase).

Data processing	Pt-KDG-aldolase	Ss-KD(P)G-aldolase
Unit Cell Dimensions (Å)	77.9, 100.2, 154.6	106.9, 106.9, 245.6
Space Group	$P22_12_1$	$P6_522$
Resolution (Å)	28.58-2.50 (2.54-2.50)	92.55-2.35 (2.43-2.35)
Completeness (%)	86.6 (83.4)	100.0 (100.0)
Rmerge	0.107 (0.333)	0.145 (2.51)
Rpim (all I+ & I-)		0.017(0.284)
Redundancy	3.8 (2.8)	75.8 (79.1)
I/σI	13.2 (2.7)	22.2 (2.7)
Number of observed reflections	877347	2692983 (269399)
Number of unique reflections	36955 (1730)	35510 (3406)
Model refinement		
Number of working set reflections	34773	35153
Number of test set reflections	1884	1686
Final Rcryst	0.175	0.187
Final Rfree	0.260	0.239
Number of non-H protein atoms	8979	4838
Number of non-H solvent atoms	340	79

RMSD bonds (Å)	0.008	0.009
RMSD angles (°)	1.18	1.00
Ramachandran plot most favoured (%)	95.8	96.74
Ramachandran plot allowed (%)	3.7	3.26

The asymmetric unit contains 4 chains, each of which folds into a classic $(\beta\alpha)_8$ TIM-barrel structure, and their structural similarity is shown by the root mean square deviation (RMSD) values of any pair of superimposed independently-refined monomers being no greater than 0.3Å. Analysis of Pt-KDG-aldolase by PISA[23] indicates that these monomers form a tetramer as a dimer of dimers, with the average dimer interface having an area of 1610Å^2 and a solvation energy for folding (ΔG_f) of -20 kcal/mol, while that between dimers in the tetramer is only 680Å^2 and -5.6kcal/mol.

Comparison with other structures in the PDB using PISA clearly identifies Pt-KDG-aldolase as a member of the dihydrodipicolinate synthetase family, having marked structural similarity with the many structures in 'Aldolase Class 1' (CATH superfamily 3.20.20.70). Several structures of KD(P)G-aldolase have been published, including those from *T. tenax* (RMSD to Pt-KDG-aldolase of 1.9Å over 259 Cα, sequence identity 21.7%), *Sulfolobus acidocaldarius* (2.0Å over 274 Cα, sequence identity 27.9%), and *S. solfataricus* (1.8Å over 259 Cα, sequence identity 24.8%). Despite the low sequence identity between these KD(P)G-aldolases, and the somewhat larger RMSD values, indicating less similarity with Pt-KDG-aldolase than the approximately 1.0Å RMSD calculated when these structures are compared to each other, the structural similarity is clear (see Fig. 3 for alignment of Ss-KD(P)GA and Pt-KDG-aldolase). All these structures have also been solved in the presence of pyruvate, glyceraldehyde or KDG, and no significant movement of the framework is seen on binding.

Overall structure of Ss-KD(P)G-aldolase in complex with KDPG.

To investigate the interactions of KDPG with a KD(P)G-aldolase, the structure of Ss-KD(P)G-aldolase in complex with KDPG was determined to 2.35Å; data processing and model refinement statistics are

given in Table 1. The overall structure is very similar to both the unliganded (1W37) and the KDG-bound (1W3N) structures (average RMSD over all 293 Cα: 0.3Å). Following refinement of the unliganded coordinates, there was clear difference density for a ligand bound in the active site, extending beyond the KDG seen in the 1W3N structure. (Fig 4B). However the density was too broad to fit a single phosphate position, and therefore the final model has KDPG in a dual conformation, with the two positions occupied approximately equally (0.52:0.48), and has been deposited in the PDB with the code 6G3Z.

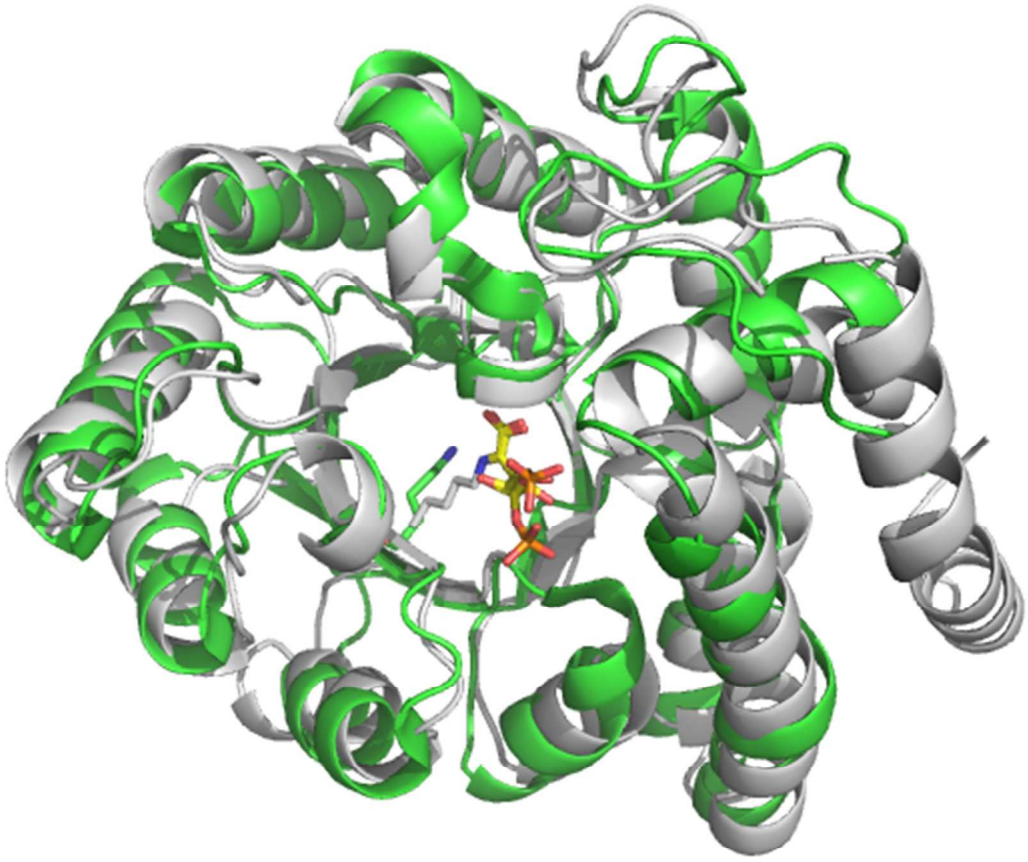

Fig 3. Cartoon representation of Ss-KD(P)G-aldolase (grey) aligned to Pt-KDG-aldolase (green) to show the overall structural similarity. The active site is marked by a stick representation of the Lysine (155 and 159 respectively) which forms the Schiff base in the catalytic reaction, and which is bound to

KDPG (yellow) in the Ss-KD(P)G-aldolase complex structure. The three N-terminal amino acids of the Pt-KDG-aldolase are removed for clarity.

Active site

The structure of Ss-KD(P)G-aldolase in complex with KDG has been described previously[13]. As noted by Theodossis et al. for this structure, in comparison with the unliganded enzyme (1W37), the majority of the Ss-KD(P)G-aldolase active site is unchanged on binding KDG, although there are minor movements of aromatic side chains (Phe 39 and Tyr 130) that are mirrored in the KDPG-bound structure. As well as these hydrophobic interactions, the same hydrogen-bonding interactions between the KDG moiety and the enzyme are seen in the two structures (the C1 acid group with the main chain of both Thr43 and Thr44 and the Thr44 side chain, O4 with Tyr130 and O6 with Tyr132) (Fig 4B). However, the KDPG-bound structure shows that the more distal part of the active site involved in phosphate interactions is somewhat less rigid; on binding KDPG, the Cα positions of Arg106, and in some monomers Glu159 (which forms salt bridges with Arg106 and Arg273; Fig 5B), are the only non-terminal Cα amino acids to move more than 1Å from their positions in the earlier structures. The movement of Arg106 can be explained through both phosphate conformations of KDPG making strong interactions (within hydrogen-bonding distance) with Arg106 from a neighbouring monomer (Fig 5B). The other interactions with the phosphates are from residues within the original monomer, conformer A interacting with Ser241 and Tyr132, while conformer B interacts with Arg237.

Through modeling studies, the interactions with Arg237, Tyr132 and Arg106 have been predicted previously in Sa-KD(P)G-aldolase (234, 105, 131)[9] and Tt-KD(P)G-aldolase (255, 150, 124)[12], being conserved across other KD(P)G aldolases, while the Ser 241, which is not conserved, had not been identified in those studies.

In all the KD(P)G-aldolase structures, the active site containing the lysine that will form the Schiff base is in a conserved position at the top of the β-barrel. As was also seen in *S. acidocaldarius* KD(P)G-aldolase when crystallised at pH 7.5, in the Pt-KDG-aldolase structure the lysine points away

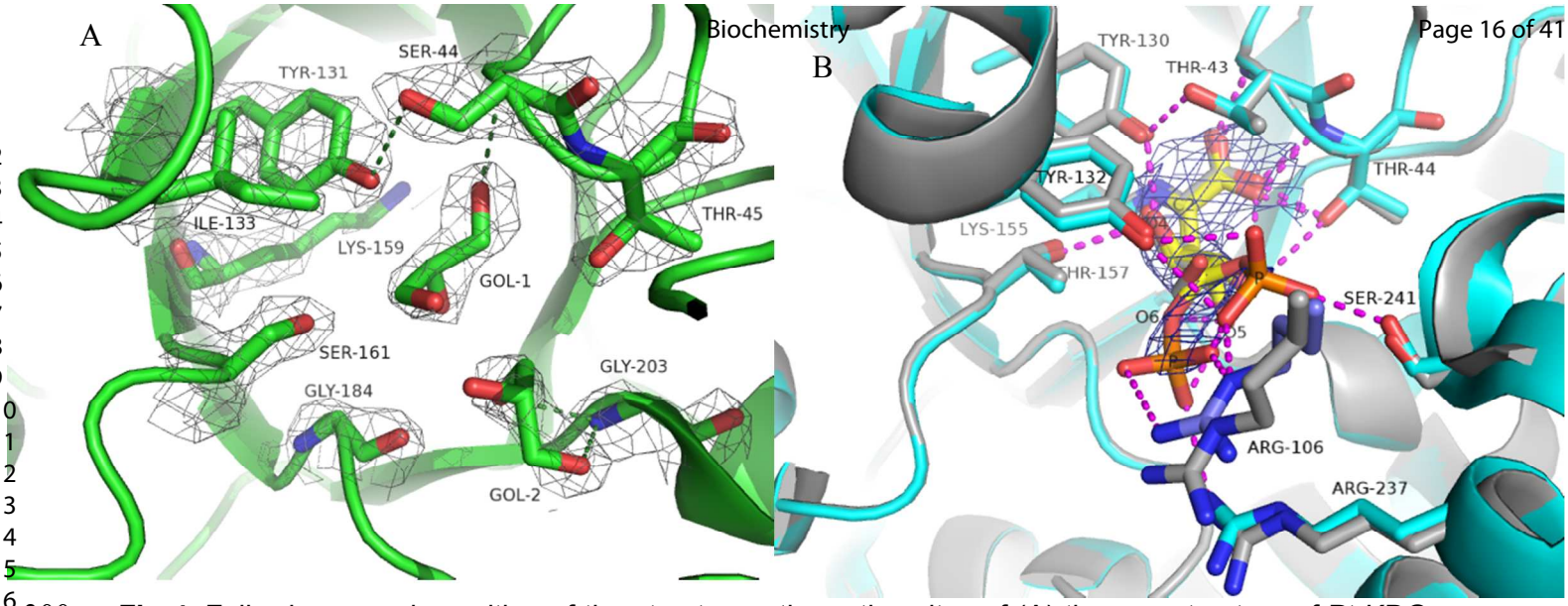

Fig 4. Following superimposition of the structures, the active sites of (A) the apo structure of Pt-KDG-aldolase (GOL are glycerol molecules) and (B) Ss-KD(P)G-aldolase with KDPG (yellow bonds) bound are shown in the same orientation with the 2FoFc electron density map for each structure, contoured at 1.5σ, restricted to that around KDPG in B for clarity. B also contains the structure of Ss-KD(P)G-aldolase with KDG bound (grey) superimposed to show the relative stasis of all but those amino acids that interact with the phosphates. The main chain cartoon containing Arg106 from a neighbouring monomer is omitted as it crosses the middle of the image. Hydrogen bonds are shown as dotted lines.

Comparison of the inner part of the binding-pocket seen in the Ss-KD(P)G-aldolase-KDPG complex structure (Fig. 4B)[20] with the Pt-KDG-aldolase active site (Fig. 4A) shows that many of the KDG interactions would be conserved in the *Picrophilus* enzyme; these comprise interactions of the pyruvate carboxylate group with Ss-KD(P)GA Thr43 (Pt-KDG-aldolase Ser44), Thr44(45), Tyr130(131), and the glyceraldehyde with Thr157(Ser161) and, via water, with Gly179(184), Thr44(45) and Ala198(Gly203). The suitability of the site to bind polar molecules in Pt-KDG-aldolase is shown by the presence of glycerol (cryoprotectant) molecules, making many of the same interactions as KDG in Ss-KD(P)G-aldolase (Fig. 4A). The interaction of the O6 of KDG with Ss-KD(P)G-aldolase Tyr132 would not be replicated in Pt-KDG-aldolase as the corresponding residue is Ile133. Both enzymes have shown promiscuity in catalyzing the cleavage of both KDG and KDGal, [4,7] so it is likely that the mechanism of action, as observed in Ss-KD(P)G-aldolase,[7] is conserved in Pt-KDG-aldolase due to

the similarities in the inner part of the binding pocket.

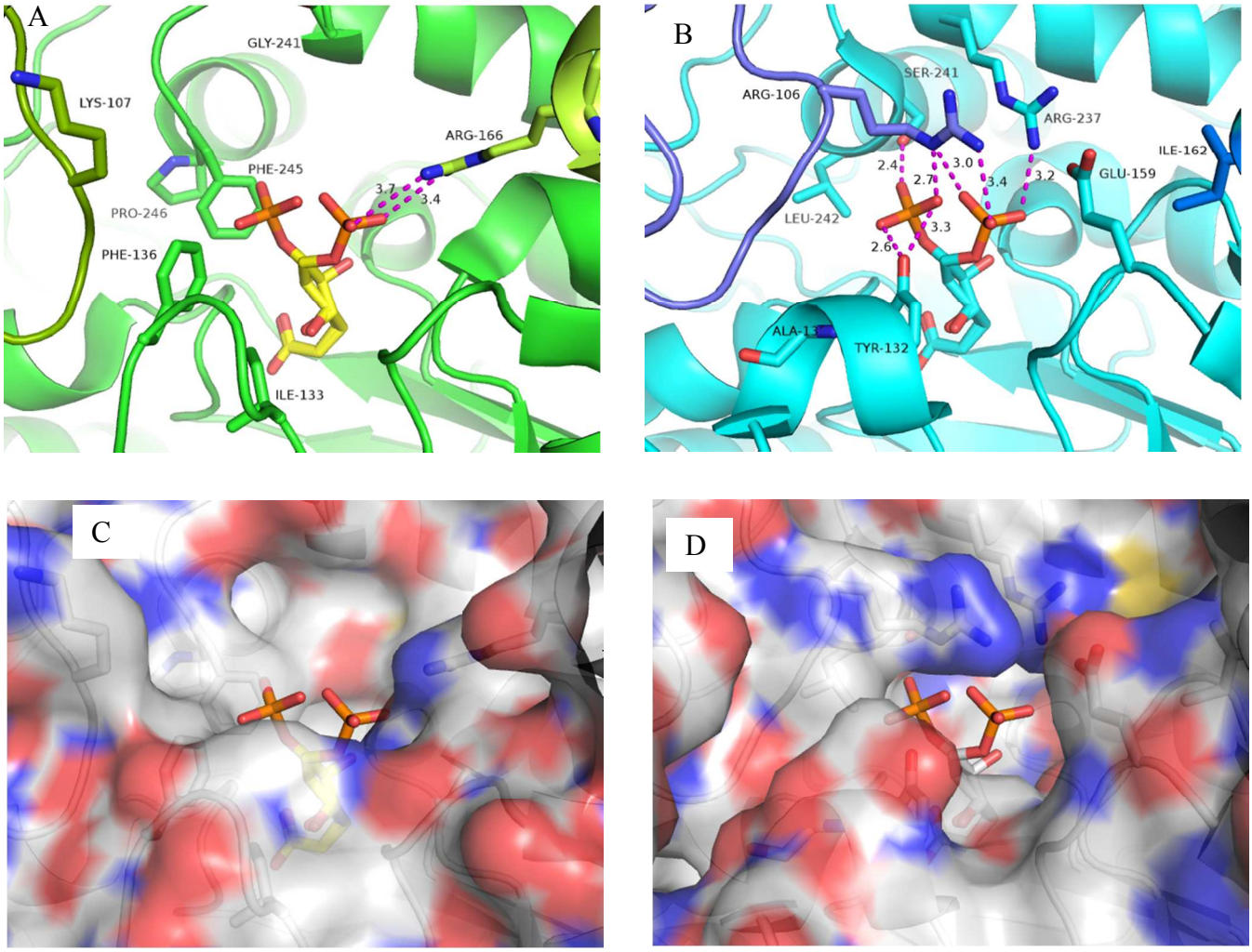

Fig 5: Analysis of interactions (shown in magenta dotted lines) made by KDPG with the active sites of Pt-KDG-aldolase (modeled on the complex between KDPG and Ss-KD(P)G-aldolase) (A,C), and those seen in Ss-KD(P)G-aldolase (B,D). (A) Stick representations of amino acids from Pt-KDG-aldolase (green) that could interact with KDPG (magenta), with those amino acids from neighbouring subunits in different shades of green. (B) A similar representation of amino acids in the Ss-KD(P)G-aldolase active site, with those from a neighbouring monomer in a different shade of blue. (C) Electrostatic surface around the catalytic site of Pt-KDG-aldolase, with positively-charged areas in blue and negative in red. (D) Electrostatic surface around the catalytic site of Ss-KD(P)G-aldolase, coloured similarly.

Unlike the other KD(P)G aldolases of known structure, the Pt-KDG-aldolase has a distinct preference for KDG over KDPG as a substrate, the catalytic efficiency with KDG being 2,000 times that with KDPG.[4] To investigate this specificity in the outer part of the binding pocket, the structure of Pt-KDG-aldolase was compared to that of Ss-KD(P)G-aldolase in complex with KDPG (Fig. 5B). None of the Ss-KD(P)G-aldolase phosphate-interacting residues is conserved in Pt-KDG-aldolase, the site of Arg237 being occupied by glycine (241), and Ser241 by phenylalanine (245), neither of which will form constructive interactions with a phosphate moiety. The main chain of Arg106 of Ss-KD(P)G-aldolase aligns with Lys107 in Pt-KDG-aldolase, also a positive amino acid, but the latter forms an interaction within its own subunit, and is not available for substrate interaction (Fig. 5A). The entrance to the active site surface is considerably more hydrophobic in Pt-KDG-aldolase (Fig 5C), although some positive charge is provided by Arg166 from the subunit on the other side (Fig. 5A), which could make longer-distance interactions with one phosphate conformation. However the other phosphate conformation would be unfavourable due to clashes, particularly with Phe 245, and the hydrophobic nature of these outer reaches of the Pt-KDG-aldolase catalytic pocket is increased further by Ile133 (Pt) instead of Tyr132 (Ss), and Phe136 (Pt) replacing Ala135 (Ss) (Fig. 5C,D). These differences are predicted to explain the lower affinity of Pt-KDG-aldolase for phosphorylated substrates.

Site-directed mutagenesis

To investigate these active-site observations further, a series of residues was swapped by site-directed mutagenesis and the resulting kinetic analyses of the variant enzymes are summarised in Table 2; kinetic analyses from selected variants are shown graphically in Supplementary Figures S1 and S2. Initial studies concentrated on three of the residues in Ss-KD(P)G-aldolase that interact with the phosphate group of the substrate KDPG, namely Arg237, Arg106 and Tyr132 . Thus Ss-KD(P)G-aldolase R237G raised the K_M for KDPG approximately 5-fold with no significant change in the V_{max}. There were no significant changes in the kinetic parameters with KDG as substrate. The reverse change in Pt-KDG-aldolase, G241R, increased the k_{cat}/K_M for KDPG 9-fold but, surprisingly, this came

from an increase in k_{cat} rather than an expected decrease in the K_M; as predicted, no change was observed in the kinetic parameters with KDG as substrate.

Table 2: Kinetic parameters determined for mutated Ss and Pt aldolases.

***S. solfataricus* KD(P)G Aldolase**

KDPG as substrate	V_{max} (U/mg)	K_M (mM)	k_{cat} (s^{-1})	k_{cat}/K_M ($s^{-1}M^{-1}$)
Native enzyme	168.4 ± 17.3	0.69 ± 0.09	97.8 ± 10.1	1.42 (± 0.24) x 10^5
R237G	174.4 ± 9.3	3.28 ± 0.28	101.1 ± 5.4	0.31 (± 0.03) x 10^5
R106I	157.6 ± 9.2	0.98 ± 0.15	91.4 ± 5.3	0.93 (± 0.15) x 10^5
Y132I	332.1 ± 43.8	0.68 ± 0.03	192.6 ± 25.3	2.83 (± 0.39) x 10^5
R106I/Y132I	141.6 ± 13.4	1.57 ± 0.33	82.1 ± 7.8	0.52 (± 0.12) x 10^5
S241F	200.4 ± 6.6	0.89 ± 0.08	116.2 ± 3.8	1.31 (± 0.13) x 10^5
S241F/L242P	114 ± 4.2	0.58 ± 0.07	66.1 ± 2.4	1.14 (±0.14) x 10^5
R106I/Y132I/S241F	85.3 ± 3.9	2.45 ± 0.20	49.5 ± 2.3	0.20 (± 0.02) x 10^5

***P. torridus* KDG Aldolase**

	V_{max} (U/mg)	K_M (mM)	k_{cat} (s^{-1})	k_{cat}/K_M ($s^{-1}M^{-1}$)
KDPG as substrate				
Native enzyme	0.785 ± 0.07	6.4 ± 1.5	0.398 ± 0.035	62.14 ± 15.6
G241R	6.77 ± 0.56	6.27 ± 0.9	3.43 ± 0.283	546.98± 90.6
KDG as substrate				
Native enzyme	62.4 ± 11.6	1.12 ± 0.3	31.6 ± 5.88	2.82 (± 0.91) x 10^4
G241R	63.4 ± 9.4	1.06 ± 0.08	32.12 ± 4.78	3.03 (± 0.51) x 10^4

In each active site of Ss-KD(P)G-aldolase, Arg106 from a neighbouring subunit interacts with the phosphate group of KDPG, and accordingly the mutation R106I raised the K_M for KDPG, although the effect was much smaller (1.4-fold) than that for R237G. The residue in the equivalent position in the *Picrophilus* enzyme is Lys107; attempts were therefore made to reposition this Lys to one similar to Arg106 in Ss-KD(P)G-aldolase. Using the sequence alignment as a guide (Fig. 6), a Pro was inserted in Pt-KDG-aldolase before Lys107, and Phe245 was changed to Ser245 as the bulky Phe appeared to be blocking the binding of the phosphate of KDPG; unfortunately, the enzyme lost over 70% of the wild-type enzyme activity, and size exclusion chromatography indicated that the enzyme was dissociating. The F245S mutant without the insertion of the Pro also had no defined oligomeric structure.

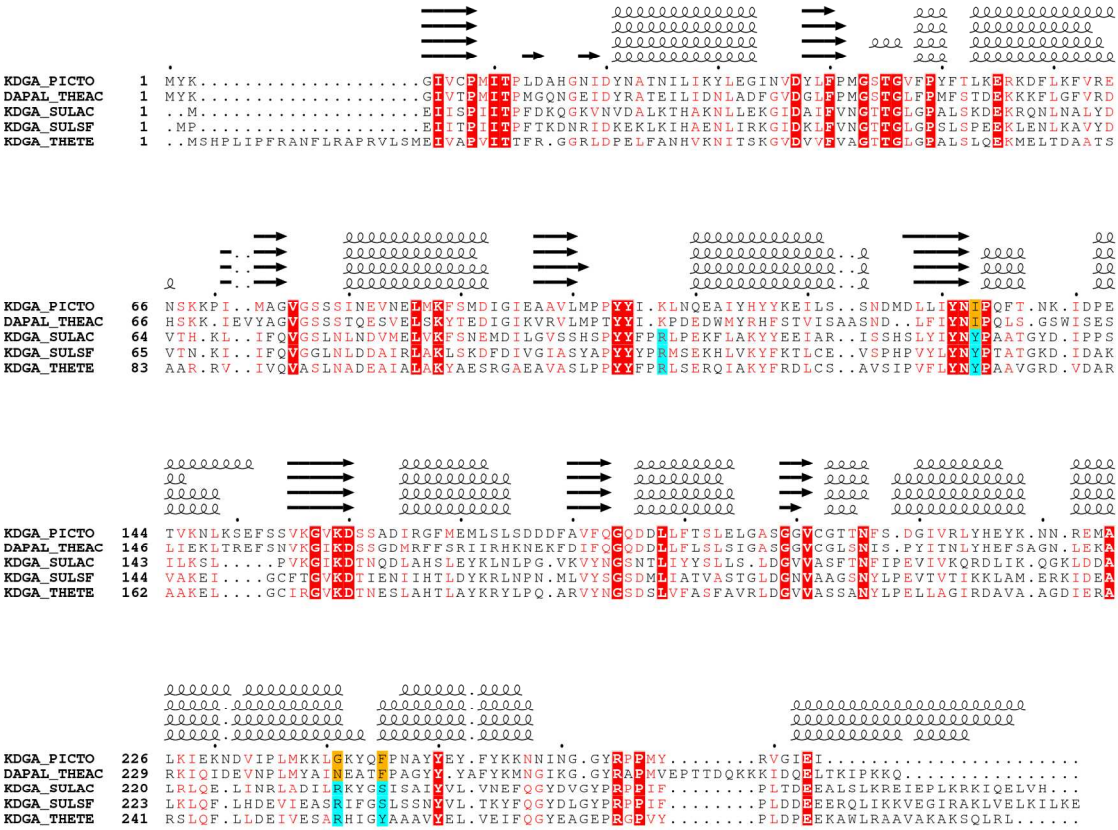

Fig 6: Structure-based sequence alignment (calculated with Expresso[24]) and displayed with Espript[25] of Pt-KDG-aldolase (KDGA_PICTO), *Thermoplasma acidophilum* KDG-aldolase (DAPAL_THEAC), *S. acidocaldarius* KD(P)G-aldolase (KDGA_SULAC), Ss-KD(P)G-aldolase (KDGA_SULSF) and *T. tenax* KD(P)G-aldolase (KDGA_THETE), with the sequences labeled with their Uniprot codes and the secondary structure depicted above the sequences. Identical amino acids are in white text on a red background; similar amino acids are in red text. The four amino acids labeled in cyan are those shown to interact with the phosphate group of KDPG in Ss-KD(P)G-aldolase, R106, Y132, R237 and S241 (Ss numbering). Those in orange are thought to make phosphate binding less likely I133, G241, F245 (Pt numbering).

Surprisingly, mutation of Y132 to Ile did not affect the K_M of Ss-KD(P)G-aldolase for KDPG, but increased k_{cat} 1.9 fold; the reason for this is perhaps that in the absence of Y132, which interacts with conformation A, the phosphate preferentially occupies the other position in the active site and the

replacement with the smaller Ile allows a more open active site. However, the mutation of Y132 in combination with R106I, affecting both phosphate binding sites, did increase the K_M two-fold over R106I alone. Mutation of I133Y in Pt-KDG-aldolase, to mimic the Ss-KD(P)G-aldolase Y132, was attempted but caused dissociation of the oligomeric structure with considerable loss of catalytic activity.

Ser241 forms a hydrogen bond with the phosphate of KDPG in Ss-KD(P)G-aldolase, whereas this position is occupied by a Phe in Pt-KDG-aldolase, which will not form hydrogen bonds and appears to obstruct the access of the phosphorylated substrate to the active site, particularly in one of the two KDPG conformations. However, the mutation S241F in Ss-KD(P)G-aldolase had only a small effect on the catalysis of KDPG. This may be because only one of the two phosphate binding conformations is affected; moreover catalysis with KDG as substrate was similarly unaffected. Also, in Pt-KDG-aldolase the Phe-containing loop takes up a different conformation from that containing S241 in Ss-KD(P)G-aldolase, possibly due to the Pro that lies underneath the Phe; consequently, the double mutant, S241F/L242P, aimed to allow the Phe to take up the *Picrophilus*-like conformation, but again little effect on the binding of KDPG was observed. However, the influence of Ser241 on the binding of KDPG was best demonstrated in the triple mutant R106I/Y132I/S241F, where a 4-fold increase in K_M was observed; that is, doubling the increase seen in the double mutant R106I/Y132I. Thus, Ser241 contributes to KDPG binding as part of a network with R106 and Y132 and together with R237, constitutes the fourth amino acid of the network.

Concluding remarks

In this communication we report the 3D structure of Pt-KDG-aldolase, which is highly specific for KDG, and the structure of Ss-KD(P)G-aldolase in complex with KDPG, where the phosphate was unexpectedly shown to bind in two conformations. By structural comparison of Pt-KDG-aldolase and KDPG-cleaving Ss-KD(P)G-aldolase, and by site-directed mutagenesis studies, a network of four amino acids composed of Arg 106, Tyr 132, Arg 237 and Ser241 was identified that contacts the phosphate of KDPG in Ss-KD(P)G-aldolase (Figure 7). This KDPG-binding network was absent in Pt-

KDG-aldolase, explaining the low catalytic efficiency of this aldolase for KDPG. The respective substrate specificities of the two aldolases for KDG and KDPG determine the two different routes of glucose degradation via non-phosphorylative or branched Entner-Doudoroff pathway in these two thermophilic archaea (Fig 1). The operation of the non-phosphorylative Entner-Doudoroff pathway in *P. torridus* is further supported by the absence of a KDG-kinase gene in this organism.

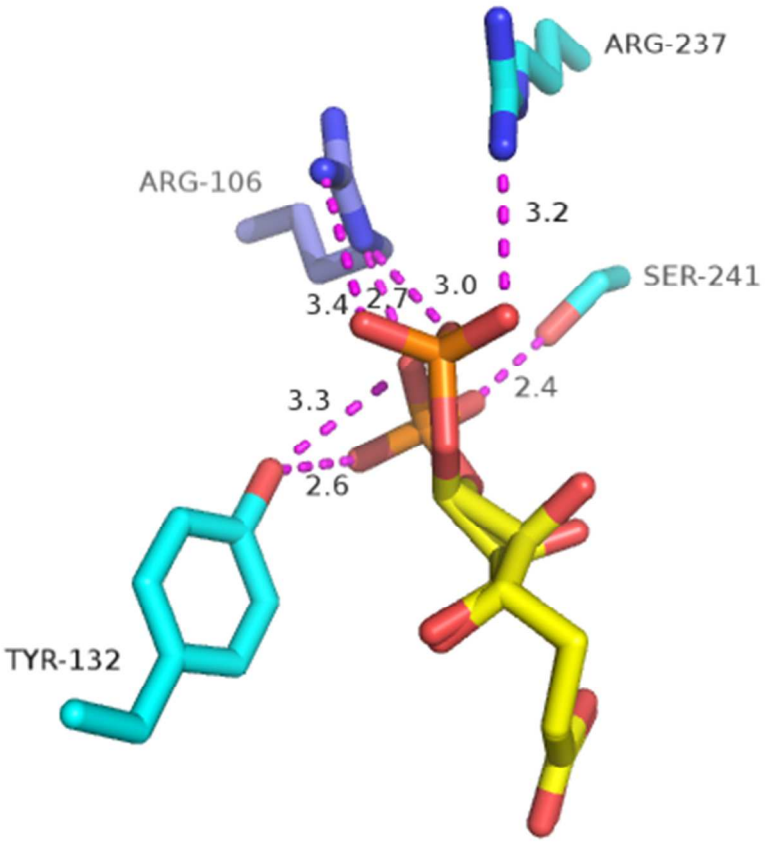

Fig 7. Interactions (magenta dotted lines with lengths in Å) of a four amino acid-network (Arg106, Tyr132, Arg237 and Ser241) predicted from structural data and shown through site-directed mutagenesis to be important for binding the phosphate group of KDPG in Ss-KD(P)G-aldolase. Ss-KD(P)G-aldolase amino acids from one monomer in cyan, from a neighbour in dark blue, and KDPG in yellow).

The presence or the absence of the four amino acid network in sequences of homologous

aldolases enables the prediction of substrate specificities of these aldolases and their functional involvement in archaeal Entner-Doudoroff pathways. The presence of the network in aldolases from *Sulfolobus acidocaldarius* and *Thermoproteus tenax* (see structure based alignment in Fig 6.) is in accordance with the kinetic properties showing high preference for KDPG over KDG; both organisms have been reported to degrade glucose via a branched Entner-Doudoroff pathway .[4,6] Furthermore, the absence of the network in the aldolase from *Thermoplasma acidophilum* is in accordance with the high specificity for KDG over KDPG and with the operation of the non-phosphorylative Entner-Doudoroff pathway in this organism.[4]

Author contributions: MR and MO produced the proteins for crystallisation. VZ crystallised Pt-KDG-aldolase and with GLT collected X-ray data on Pt-KDG-aldolase crystals; SJC solved and refined the Pt-KDG-aldolase crystal structure and also crystallised and solved the structure of the Ss-KD(P)G-aldolase complex with KDPG. MO and UJ performed the mutagenesis experiments and MJD, PS, and UJ analysed the enzyme kinetic data . PS initiated the project and SJC, PS, MJD and UJ have been involved in writing the paper.

Acknowledgements

Initial work of site-directed mutagenesis studies was performed by Jasmin Gille as part of her bachelor thesis (Christian-Albrechts-Universität Kiel). Refinement of the Pt-KDG-aldolase structure was carried out as part of the work submitted by Alexandros Priftis for an MRes in Protein Structure and Function at the University of Bath. The authors would like to thank Diamond Light Source for beamtime (proposal mx17212-8), and Gyles Cozier, William Bradshaw, Shalini Iyer and the staff of beamline i04 for assistance with data collection. This research received no specific grant from any funding agency in the public, commercial or not-for-profit sectors. None of the authors have any real or perceived conflicts of interest.

Supporting Information. Kinetic analyses of wild-type and mutant aldolases from Sulfolobus (Figure S1) and Picrophilus (Figure S2).

References

1. Bräsen, C.; Esser, D.; Rauch, B.; Siebers, B. (2014) Carbohydrate metabolism in Archaea: current insights into unusual enzymes and pathways and their regulation. Microbiol. Mol. Biol. Rev. 78, 89-175.

2. Danson, M.J.; Lamble, H.J.; Hough, D.W. (2007) Central metabolism. in *Archaea: Molecular and Cellular Biology* (Cavicchioli R. Ed.), p 260-287, ASM Press, Washington DC.

3. Siebers, B.; Schönheit, P. (2005). Unusual pathways and enzymes of central carbohydrate metabolism in Archaea. Curr. Opin. Microbiol. 8, 95-705.

4. Reher, M.; Fuhrer, T.; Bott, M.; Schönheit, P. (2010) The nonphosphorylative Entner-Doudoroff pathway in the thermoacidophilic euryarchaeon *Picophilus torridus* involves a novel 2-keto-3-deoxygluconate-specific aldolase. J. Bacteriol. 192, 964-974.

5. Angelov, A.; Fütterer, O.; Valerius, O.; Braus, G.H.; Liebl, W. (2005) Properties of the recombinant glucose/galactose dehydrogenase from the extreme thermoacidophile, *Picrophilus torridus*. FEBS J. 272, 1054-1062.

6. Ahmed, H.; Ettema, T.J.G.; Tjaden, B.; Geerling, A.C.M.; van der Oost, J.; Siebers, B. (2005) The semi-phosphorylative Entner-Doudoroff pathway in hyperthermophilic archaea - a re-evaluation. Biochem J. 390, 529-540.

7. Lamble, H.J.; Theodossis, A.;. Milburn, C.C.; Taylor, G.L.;. Bull, S.D.; Hough, D.W.; Danson, M.J. (2005) Promiscuity in the part-phosphorylative Entner-Doudoroff pathway of the archaeon *Sulfolobus solfataricus*. FEBS Lett. 579, 6865-6869.

8. Lamble, H.J.; Heyer, N.I.; Bull, S.D.; Hough, D.W.; Danson, M.J. (2003) Metabolic pathway promiscuity in the archaeon *Sulfolobus solfataricus* revealed by studies on glucose dehydrogenase and 2-keto-3-deoxygluconate aldolase. J. Biol. Chem. 278, 34066-34072.

9. Wolterink-van Loo, S.; van Eerde, A.; Siemerink, M.A.J.; Akerboom, J.; Dijkstra, B.W.; van der Oost, J. (2007) Biochemical and structural exploration of the catalytic capacity of *Sulfolobus* KDG aldolases.

Biochem. J. 403, 421-430.

10. Sutter, J.M.; Tästensen, J.B.; Johnsen, U.; Soppa, J.; Schönheit, P. (2016) Key enzymes of the semiphosphorylative Entner-Doudoroff pathway in the haloarchaeon *Haloferax volcanii*: characterization of Glucose Dehydrogenase, Gluconate Dehydratase, and 2-Keto-3-Deoxy-6-Phosphogluconate Aldolase. J. Bacteriol. 198, 2251-2262.

11. Allard, J.; Grochulski, P.; Sygusch, J. (2001) Covalent intermediate trapped in 2-keto-3-deoxy-6-phosphogluconate (KDPG) aldolase structure at 1.95-Å resolution. Proc. Natl. Acad. Sci. USA 98, 3679-3684.

12. Pauluhn, A.; Ahmed, H.; Lorentzen, E.; Buchinger, S.; Schomburg, D.; Siebers, B.; Pohl, E. (2008) Crystal structure and stereochemical studies of KD(P)D aldolase from *Thermoproteus tenax*. Prot. Struct. Func. Bioinf. 72, 35-43.

13. Theodossis, A.; Walden, H.; Westwick, E.J.; Connaris, H.; Lamble, H.J.; Hough, D.W.; Danson, M.J.; Taylor, G.L. (2004) The structural basis for substrate promiscuity in 2-keto-3-deoxygluconate aldolase from the Entner-Doudoroff pathway in *Sulfolobus solfataricus*. J. Biol. Chem. 279, 43886-43892.

14. Otwinowski, Z.; Minor, W. (1997). Processing of X-ray diffraction data collected in oscillation modein *Methods Enzymol. 276 Macromolecular Crystallography, Part A* (Carter, C.W. Jr, Sweet, R.M. Ed), , p307-326, Academic Press, New York.

15. Long, F.; Vagin, A.A.; Young, P.; Murshudov, G.N. (2008) BALBES: a molecular-replacement pipeline. Acta Crystallogr. D64, 125-132.

16. Blagova, E.; Levdikov, V.; Milioti, N.; Fogg, M.J.; Kalliomaa, A.K.; Brannigan, J.A.; Wilson, K.S.; Wilkinson, A.J. (2006) Crystal structure of dihydrodipicolinate synthase (BA3935) from *Bacillus anthracis* at 1.94Å resolution. Prot. Struct. Func. Bioinf. 62, 297-301.

17. Emsley, P.; Lohkamp, B.; Scott, W.; Cowtan, K. (2010). Features and Development of Coot. Acta Crystallogr. D 66, 486-501.

18. Adams, P.D.; Afonine, P.V.; Bunkoczi, G.; Chen, V.B.; Davis, I.W.; Echols, N.; Headd, J.J.; Hung, L.W.; Kapral, G.J.; Grosse-Kunstleve, R.W.; McCoy, A.J.; Moriarty, N.W.; Oeffner, R.; Read, R.J.; Richardson, D.C.; Richardson, J.S.; Terwilliger, T.C.; Zwart, P.H. (2010) PHENIX: a comprehensive Python-based system for macromolecular structure solution. Acta Crystallogr. D 66, 213-221.

19. Winter, G.; Waterman, D.G.; Parkhurst, J.M.; Brewster, A.S.; Gildea, R.J.; Gerstel, M.; Fuentes-Montero, L.; Vollmar, M.; Michels-Clark, T.; Young, I.D.; Sauter, N.K.; Evans, G. (2018) DIALS: implementations and evaluation of a new integration package. Acta Crystallogr. D74, 85-97.

20. Evans, P.R.; Murshudov, G.N. (2013) How good are my data and what is the resolution?. Acta Crystallogr. D69, 1204-14.

21. Lebedev, A.A.; Young, P.; Isupov, M.N.; Moroz, O.V.; Vagin, A.A.; Murshudov, G.N. (2012) *Jigand*: A graphical tool for the CCP4 template-restraint library. Acta Crystallogr. D68, 431-440.

22. The PyMOL Molecular Graphics System, Version 1.8 Schrödinger, LLC. .2015.

23. Krissinel, E.; Henrick, K. (2007) Inference of macromolecular assemblies from crystalline state. J Mol. Biol. 372, 774-797.

24. Armougom, F.; Moretti, S.; Poirot, O.; Audic, S.; Dumas, P.; Schaeli, B.; Keduas, K.; Notredame, C. (2006) Expresso: automatic incorporation of structural information in multiple sequence alignments using 3D-Coffee. Nucleic Acids Res. 34, W604-608.

25. Robert, X.; Gouet, R. (2014). Deciphering key features in protein structures with the new ENDscript server. Nucleic Acids Res. 42: W320-W324.

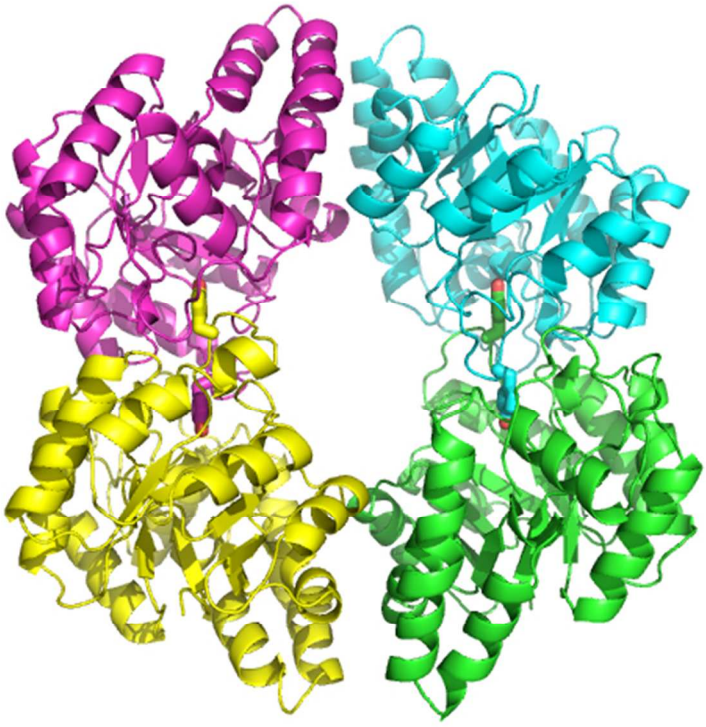

Figure 2: The structure of Pt-KDG-aldolase in cartoon representation, with each monomer in a different colour. The Ramachandran-outliers Tyr 105 are shown in stick form, and can be seen to protrude into a neighbouring molecule as part of the larger dimer interface, the perpendicular tetramer interface being less extensive.

54x40mm (300 x 300 DPI)

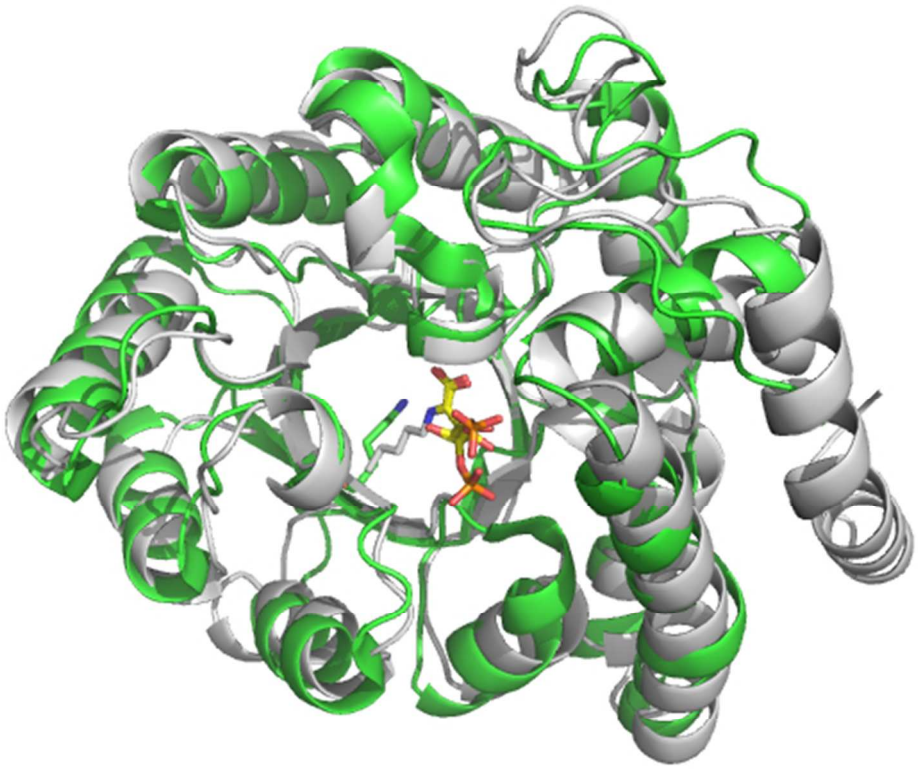

Fig 3. Cartoon representation of Ss-KD(P)G-aldolase (grey) aligned to Pt-KDG-aldolase (green) to show the overall structural similarity. The active site is marked by a stick representation of the Lysine (155 and 159 respectively) which forms the Schiff base in the catalytic reaction, and which is bound to KDPG (yellow) in the Ss-KD(P)G-aldolase complex structure. The three N-terminal amino acids of the Pt-KDG-aldolase are removed for clarity.

47x40mm (300 x 300 DPI)

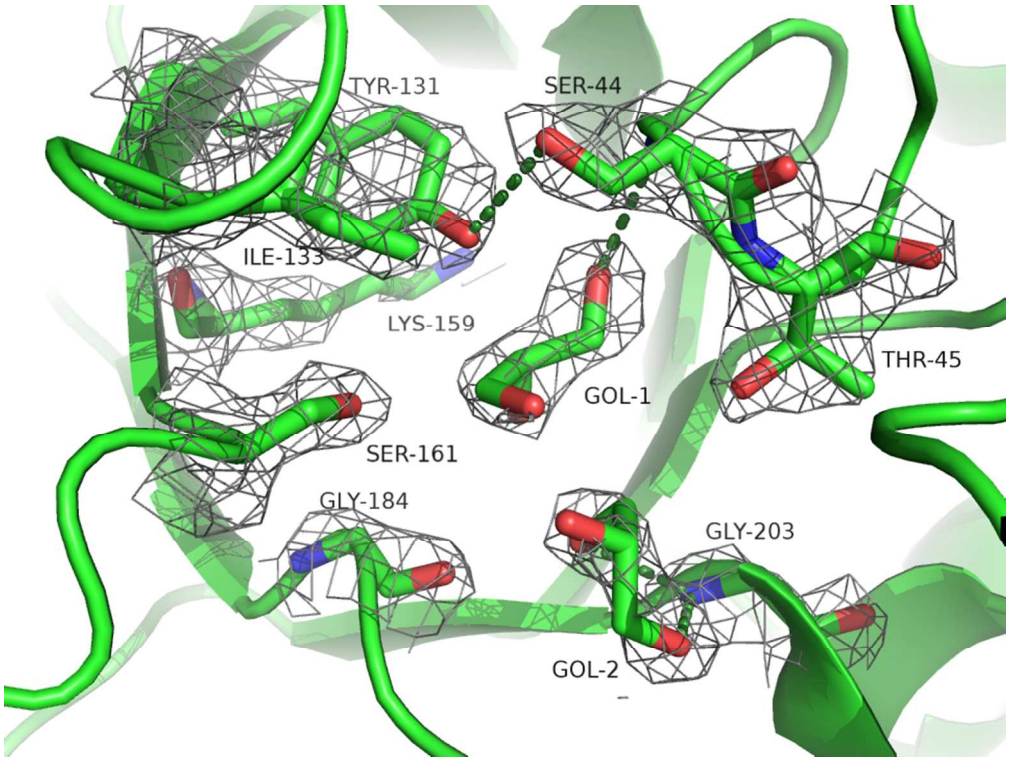

Figure 4A

81x60mm (300 x 300 DPI)

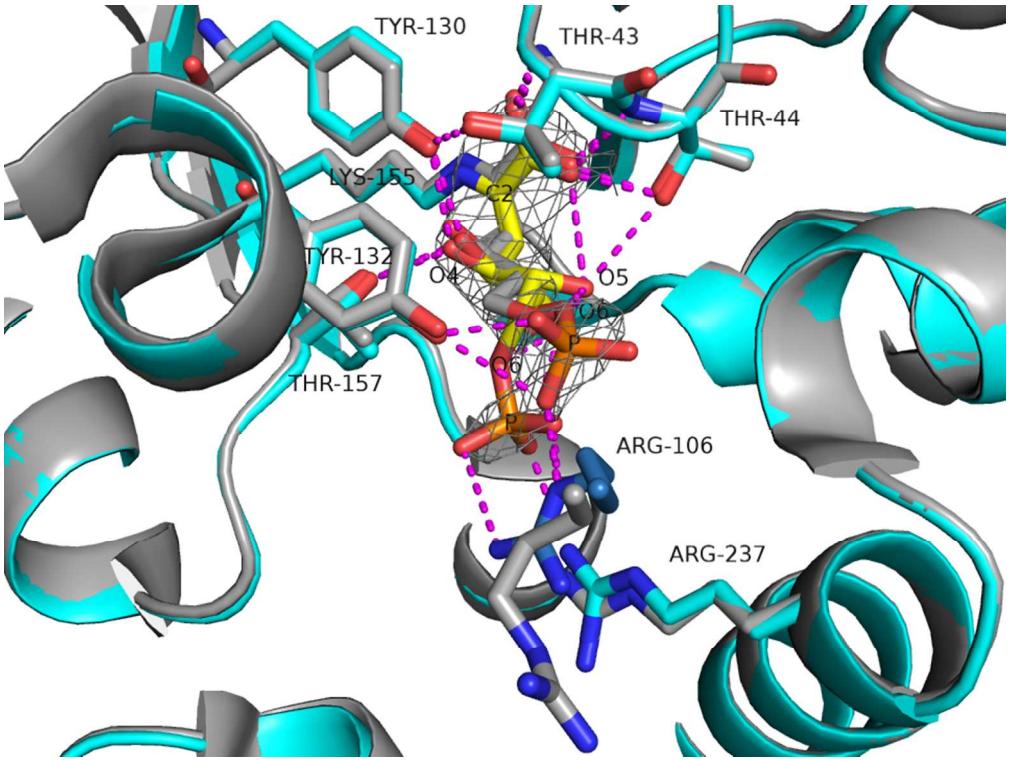

Fig 4. Following superimposition of the structures, the active sites of (A) the apo structure of Pt-KDG-aldolase (GOL are glycerol molecules) and (B) Ss-KD(P)G-aldolase with KDPG (yellow bonds) bound are shown in the same orientation with the 2FoFc electron density map for each structure, contoured at 1.5σ restricted to that around KDPG in B for clarity. B also contains the structure of Ss-KD(P)G-aldolase with KDG bound (grey) superimposed to show the relative stasis of all but those amino acids that interact with the phosphates. The main chain cartoon containing Arg106 from a neighbouring monomer is omitted as it crosses the middle of the image. Hydrogen bonds are shown as dotted lines.

81x60mm (300 x 300 DPI)

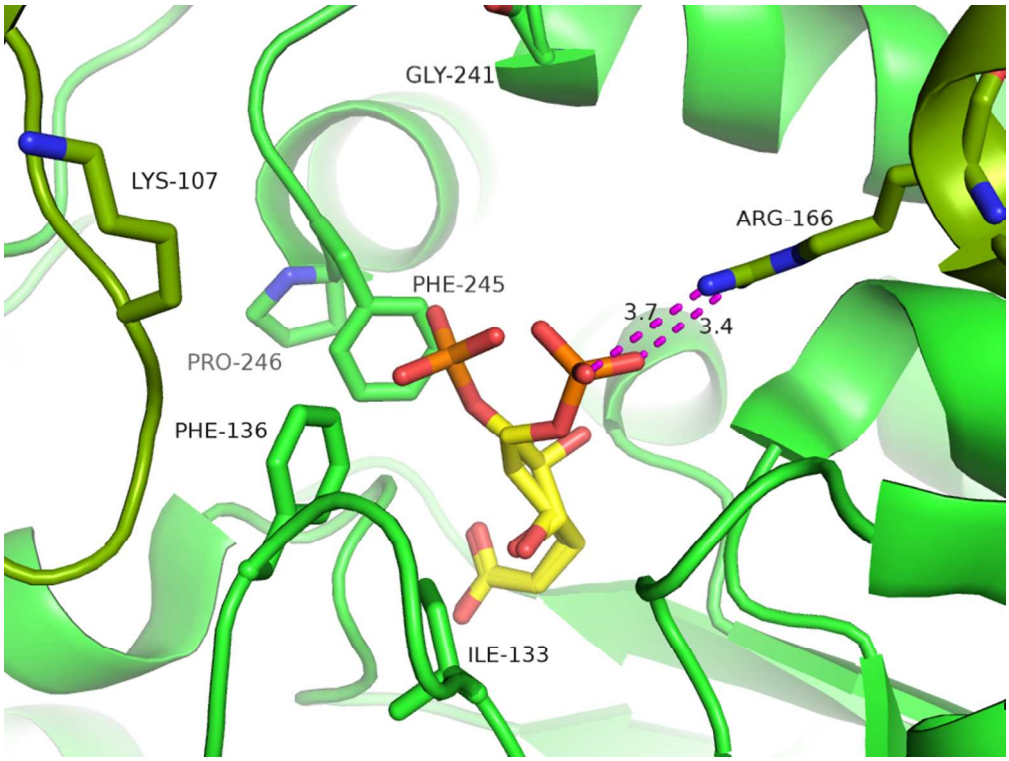

Figure 5A

81x60mm (300 x 300 DPI)

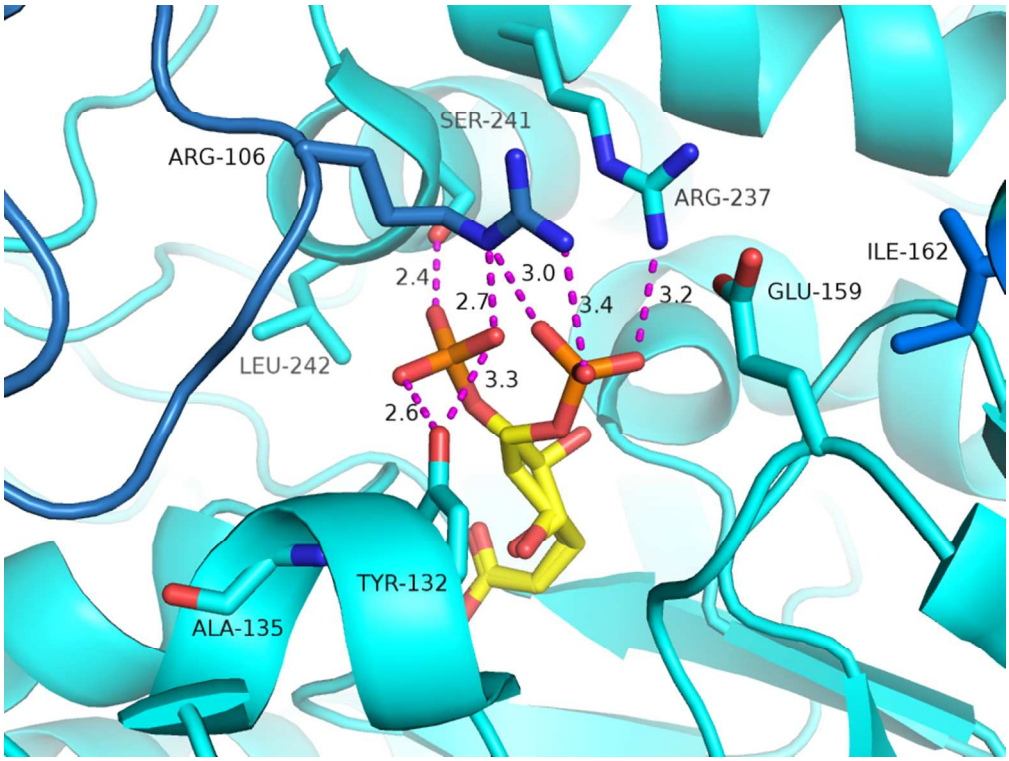

Figure 5B

81x60mm (300 x 300 DPI)

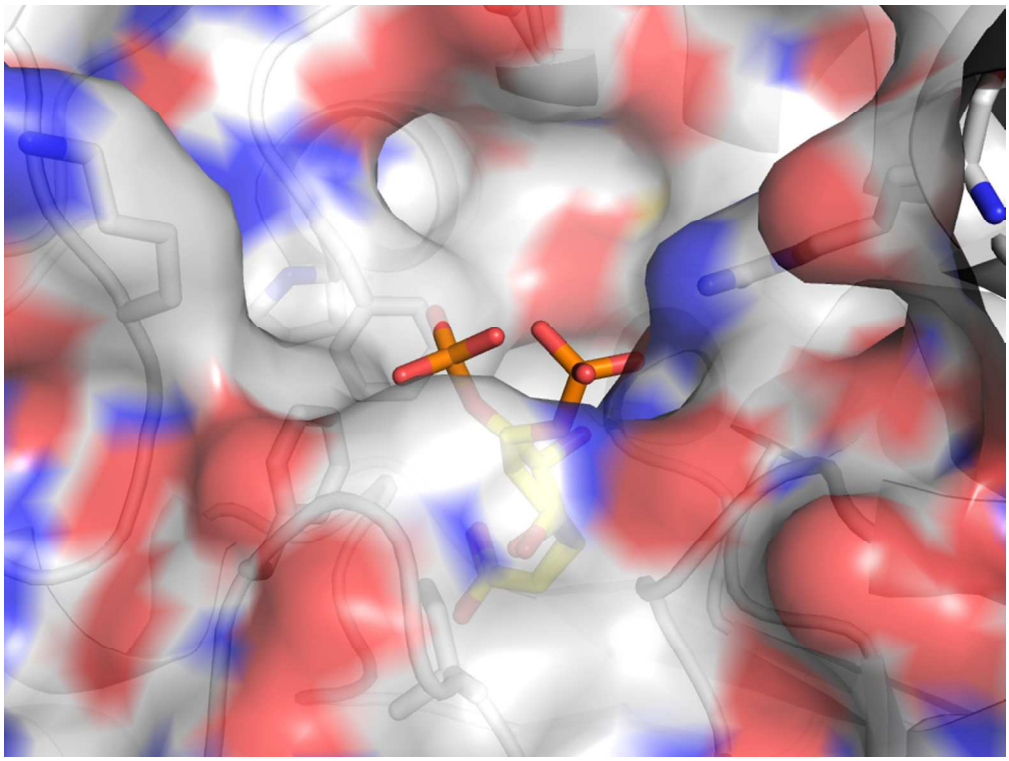

Figure 5C

81x60mm (300 x 300 DPI)

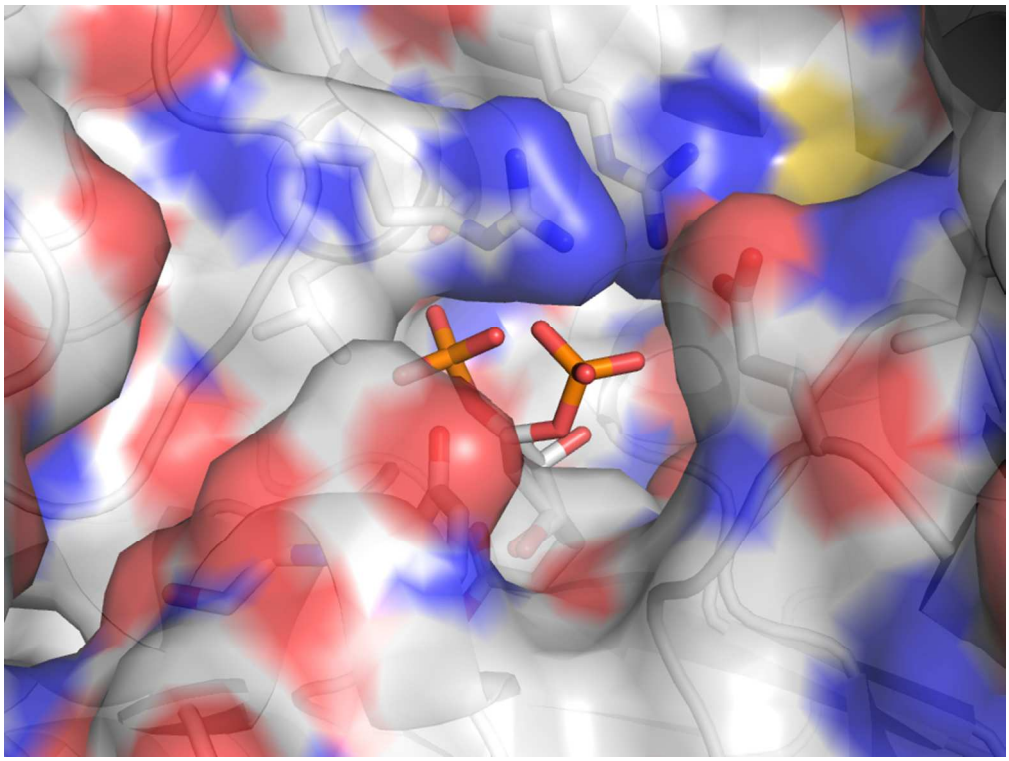

Fig 5: Analysis of interactions (shown in magenta dotted lines) made by KDPG with the active sites of Pt-KDG-aldolase (modeled on the complex between KDPG and Ss-KD(P)G-aldolase) (A,C), and those seen in Ss-KD(P)G-aldolase (B,D). (A) Stick representations of amino acids from Pt-KDG-aldolase (green) that could interact with KDPG (magenta), with those amino acids from neighbouring subunits in different shades of green. (B) A similar representation of amino acids in the Ss-KD(P)G-aldolase active site, with those from a neighbouring monomer in a different shade of blue. (C) Electrostatic surface around the catalytic site of Pt-KDG-aldolase, with positively-charged areas in blue and negative in red. (D) Electrostatic surface around the catalytic site of Ss-KD(P)G-aldolase, coloured similarly.

81x60mm (300 x 300 DPI)

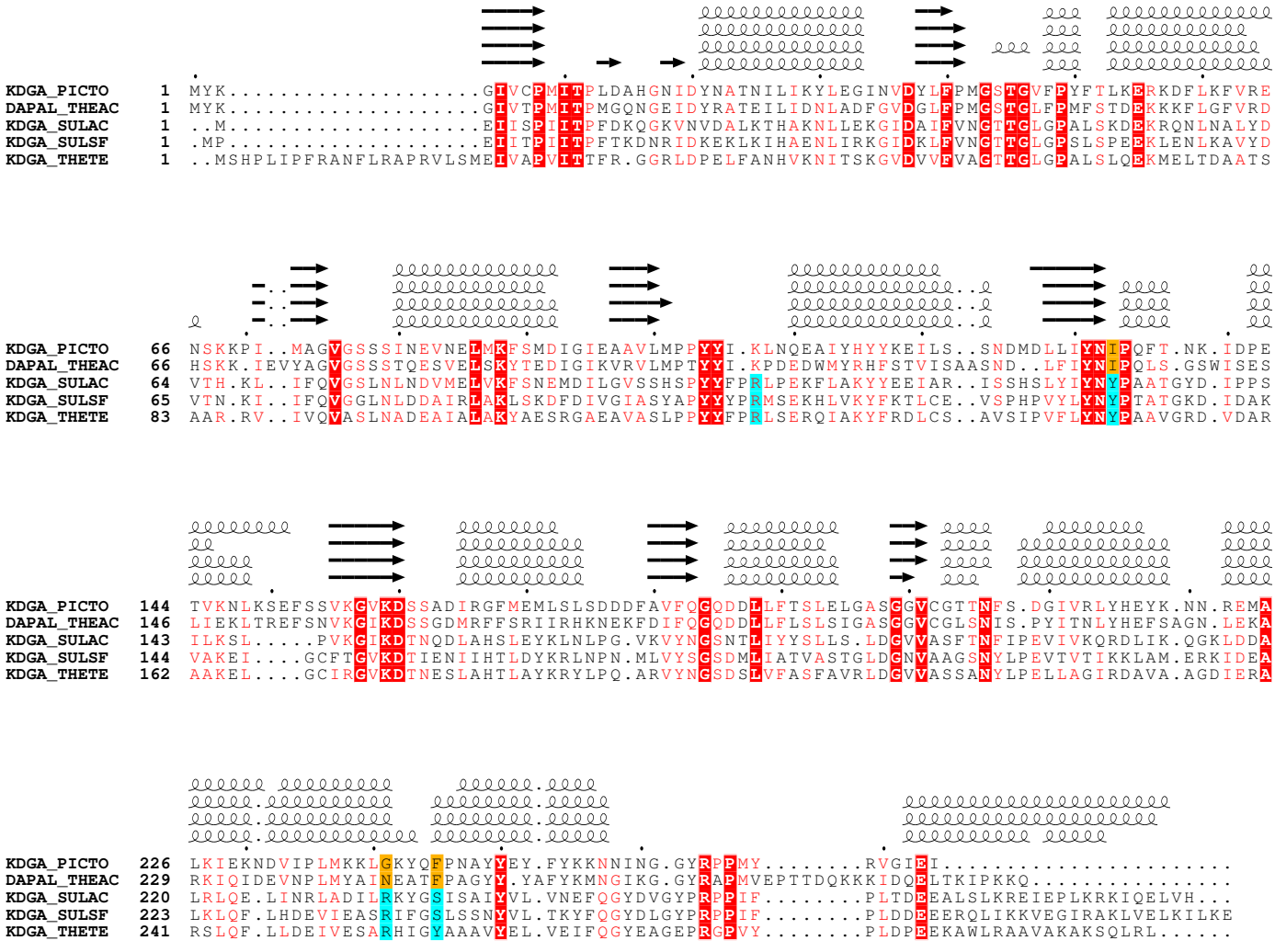
KDGA_PICTO 1 MYK.....GIVCPMITPLDAHGNIDYNATNILIKYLEGINVDYLFPMGSTGVFPYFTLKERKDFLKFVRE
DAPAL_THEAC 1 MYK.....GIVTPMITPMGQNGEIDYRATEILIDNLADFGVDGLFPMGSTGLFPMFSTDEKKKFLGFVRD
KDGA_SULAC 1 ..M.....EIISPIITPFDKQGKVNVDALKTHAKNLLEKGIDAIFVNGTTGLGPALSKDEKRQNLNALYD
KDGA_SULSF 1 .MP.....EIITPIITPFTKDNRIDKEKLKIHAENLIRKGIDKLFVNGTTGLGPSLSPEEKLENLKAVYD
KDGA_THETE 1 ..MSHPLIPFRANFLRAPRVLSMEIVAPVITTFR.GGRLDPELFANHVKNITSKGVDVVFVAGTTGLGPALSLQEKMELTDAATS
KDGA_PICTO 66 NSKKPI..MAGVGSSSINEVNELMKFSMDIGIEAAVLMPPYYI.KLNQEAIYHYYKEILS..SNDMDLLIYNIPQFT.NK.IDPE
DAPAL_THEAC 66 HSKK.IEVYAGVGSSSTQESVELSKYTEDIGIKVRVLMPTYYI.KPDEDWMYRHFSTVISAASND..LFIYNIPQLS.GSWISES
KDGA_SULAC 64 VTH.KL..IFQVGSLNLNDVMELVKFSNEMDILGVSSHSPYYFPRLPEKFLAKYYEEIAR..ISSHSLYIYNYPAATGYD.IPPS
KDGA_SULSF 65 VTN.KI..IFQVGGLNLDDAIRLAKLSKDFDIVGIASYAPYYYPRMSEKHLVKYFKTLCE..VSPHPVYLYNYPTATGKD.IDAK
KDGA_THETE 83 AAR.RV..IVQVASLNADEAIALAKYAESRGAEAVASLPPYYFPRLSERQIAKYFRDLCS..AVSIPVFLYNYPAAVGRD.VDAR
KDGA_PICTO 144 TVKNLKSEFSSVKGVKDSSADIRGFMEMLSLSDDDFAVFQGQDDLLFTSLELGASGGVCGTTNFS.DGIVRLYHEYK.NN.REMA
DAPAL_THEAC 146 LIEKLTREFSNVKGIKDSSGDMRFFSRIIRHKNEKFDIFQGQDDLLFLSLSIGASGGVCGLSNIS.PYITNLYHEFSAGN.LEKA
KDGA_SULAC 143 ILKSL.....PVKGIKDTNQDLAHSLEYKLNLPG.VKVYNGSNTLIYYSLLS.LDGVVASFTNFIPEVIVKQRDLIK.QGKLDDA
KDGA_SULSF 144 VAKEI....GCFTGVKDTIENIIHTLDYKRLNPN.MLVYSGSDMLIATVASTGLDGNVAAGSNYLPEVTVTIKKLAM.ERKIDEA
KDGA_THETE 162 AAKEL....GCIRGVKDTNESLAHTLAYKRYLPQ.ARVYNGSDSLVFASFAVRLDGVVASSANYLPELLAGIRDAVA.AGDIERA
KDGA_PICTO 226 LKIEKNDVIPLMKKLGKYQFPNAYYEY.FYKKNNING.GYRPPMY.....RVGIEI.....
DAPAL_THEAC 229 RKIQIDEVNPLMYAINEATFPAGYY.YAFYKMNGIKG.GYRAPMVEPTTDQKKKIDQELTKIPKKQ.....
KDGA_SULAC 220 LRLQE.LINRLADILRKYGSISAIYVL.VNEFQGYDVGYPRPPIF.....PLTDEEALSLKREIEPLKRKIQELVH...
KDGA_SULSF 223 LKLQF.LHDEVIEASRIFGSLSSNYVL.TKYFQGYDLGYPRPPIF.....PLDDEEERQLIKKVEGIRAKLVELKILKE
KDGA_THETE 241 RSLQF.LLDEIVESARHIGYAAAVYEL.VEIFQGYEAGEPRGPVY.....PLDPEEKAWLRAAVAKAKSQLRL.....

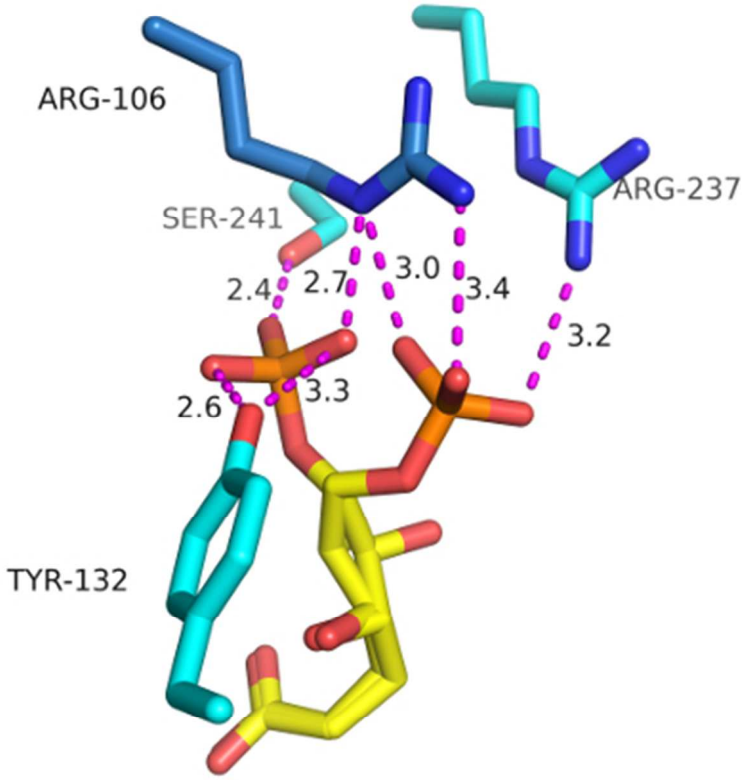

Fig 7. Interactions (magenta dotted lines with lengths in Å) of a four amino acid-network (Arg106, Tyr132, Arg237 and Ser241) predicted from structural data and shown through site-directed mutagenesis to be important for binding the phosphate group of KDPG in Ss-KD(P)G-aldolase. Ss-KD(P)G-aldolase amino acids from one monomer in cyan, from a neighbour in dark blue, and KDPG in yellow).

44x44mm (300 x 300 DPI)

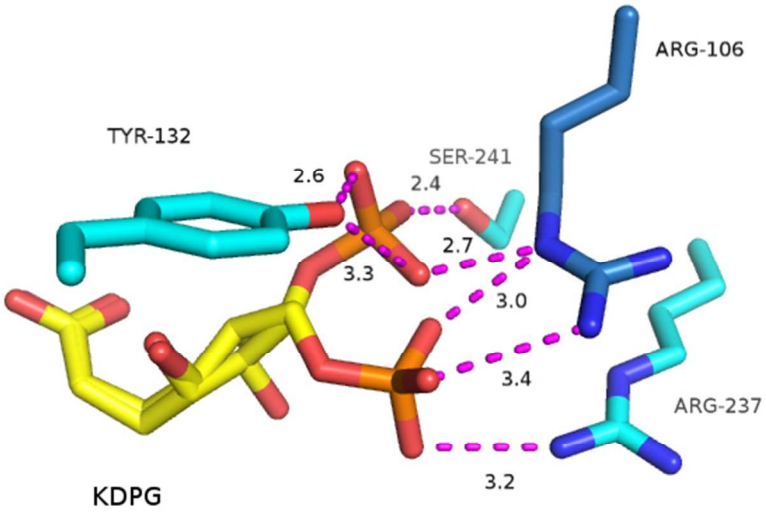

Table of Contents graphic (Figure 7 rotated)

60x33mm (300 x 300 DPI)